

Kinetic Studies on the Thermal *Cis*–*Trans* Isomerization of 1,3-Diphenyltriazene in Aqueous Solution. Effects of Acids and Bases

Mónica Barra* and Nan Chen

Guelph-Waterloo Centre for Graduate Work in Chemistry and Biochemistry, Waterloo Campus, University of Waterloo, Waterloo, Ontario, Canada N2L 3G1

mbarra@sciborg.uwaterloo.ca

Received April 19, 2000 (Revised Manuscript Received June 27, 2000)

The thermal *cis*-to-*trans* isomerization of 1,3-diphenyltriazene (**DPT**) has been investigated in buffered aqueous solutions by means of laser-flash photolysis techniques. The *cis*-to-*trans* isomerization process is found to be catalyzed by general acids and general bases as a result of acid/base-promoted 1,3-prototropic rearrangements. Acid catalysis is attributed to rate-limiting proton transfer to the nitrogen–nitrogen double bond of *cis*-**DPT**, whereas base catalysis is attributed to rate-limiting base-promoted ionization of the amino nitrogen of *cis*-**DPT** leading to the isomerization. In addition, a process ascribed to the interconversion of *cis* rotamers through hindered rotation around the nitrogen–nitrogen single bond is also observed; at high pH this process becomes rate-limiting.

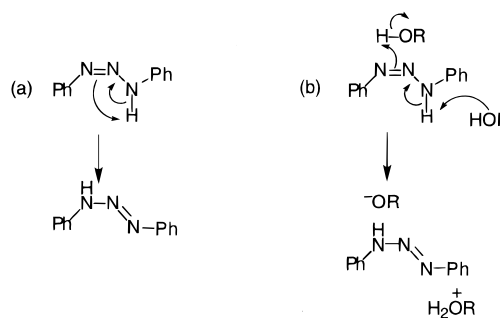
Introduction

The study of compounds able to undergo reversible isomerization around double bonds has been actively pursued in recent years, as a result of the potential application of these materials in information storage systems and (photochemical) switching devices.¹

Triazenes, compounds characterized by having a diazomino group, appear to always adopt the *trans* configuration in the ground state (as shown by X-ray diffraction and dipole moment measurements);² nonetheless, triazenes are also known to exhibit (photoinduced) reversible *cis*–*trans* isomerism. In contrast to the case of azo compounds, mechanistic investigations on the *cis*–*trans* isomerization of triazenes are very limited.^{3,4} In this regard, it has been shown that the rate of the thermal *cis*-to-*trans* isomerization of 1,3-diphenyltriazene (**DPT**) depends strongly on the polarity of the solvent, the rate increasing as the polarity of the medium increases.^{3a,4} Two mechanisms (Scheme 1) have been proposed for the *cis*-to-*trans* isomerization of **DPT** in organic solvents:^{3a,4} (a) an intramolecular 1,3-hydrogen shift (nonpolar solvents) and (b) a solvent-assisted 1,3-hydrogen shift in which protic solvent molecules act as proton donors and proton acceptors leading to the isomerization.

The present study was undertaken in an attempt to improve our understanding of the thermal *cis*-to-*trans* isomerization mechanism of triazenes, particularly with regard to the role of acids and bases as potential catalyts. Thus, time-resolved laser-flash photolysis tech-

Scheme 1



niques have been applied to the analysis of the isomerization mechanism of **DPT** in aqueous solutions at $6 < \text{pH} < 14$.

Results

Laser excitation at 355 nm of **DPT** in buffered aqueous solutions leads to instantaneous bleaching followed by complete recovery of the initial absorbance of the solutions (Figure 1 is representative). The instantaneous bleaching, ascribed to photoinduced *trans*-to-*cis* isomerization, would indicate that the extinction coefficients of the *cis* isomer in the visible region are lower than those corresponding to the *trans* form. This observation is in agreement with the UV–vis absorption spectrum calculated for *cis*-**DPT** in poly(methyl methacrylate) film, which shows that at $\lambda > 350$ nm *cis*-**DPT** has lower absorptivity than *trans*-**DPT**.^{3b} On the other hand, the complete recovery would indicate that the entire photoinduced process is reversible, and it is ascribed to the thermal *cis*-to-*trans* isomerization, in agreement with data in the literature.^{3a,4}

Recovery traces were collected at different pHs using series of solutions at constant buffer ratio (and, hence, constant pH) but varying total buffer concentration.

(1) Martin, P. J. in *An Introduction to Molecular Electronics*; Petty, M. C., Bryce, M. R., Bloor, D., Eds.; Oxford University Press: New York, 1995; Chapter 6.

(2) Benson, F. R. *The High Nitrogen Compounds*; John Wiley & Sons: New York, 1984; Chapter 3.

(3) Baro, J.; Dudek, D.; Luther, K.; Troe, J. *Ber. Bunsen-Ges. Phys. Chem.* **1983**, *87*, (a) 1155; (b) 1161.

(4) Scaiano, J. C.; Chen, C.; McGarry, P. F. *J. Photochem. Photobiol. A: Chem.* **1991**, *62*, 75.

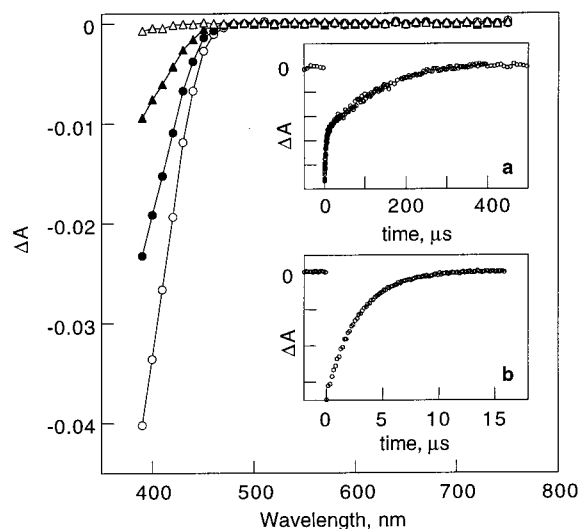


Figure 1. Transient absorption spectra for **DPT** (pH = 13, NaOH buffer) obtained 0.72 μs (○), 2.72 μs (●), 5.92 μs (▲), and 13.5 μs (△) after laser pulse. Inset: kinetic traces recorded at 390 nm at (a) pH = 6.85 (0.01 M phosphate buffer) and (b) 0.0983 M NaOH buffer.

Recovery traces (e.g., Figure 1 inset) were very well reproduced by one or two exponential terms, depending on pH (see below). Deaerating the solutions showed no measurable effect in any case.

Phosphate Buffer (6.0 < pH < 7.6). Recovery traces are adequately described by two exponential terms with preexponential factors independent of pH and buffer concentration. The observed rate constant corresponding to the faster process (k_{obs}^f) is also found to be independent of pH and buffer concentration (Table S1)⁵ and has an average value of $(3.1 \pm 0.1) \times 10^5 \text{ s}^{-1}$. The observed rate constant corresponding to the slower process (k_{obs}^s), on the other hand, increases as proton concentration and buffer concentration increase as well (Table S2),⁵ which is indicative of acid catalysis. Plots of k_{obs}^s vs buffer concentration are fairly linear (Figure 2 is representative); hence, the data obey the linear rate law of eq 1, in which k_{C} is the catalytic rate coefficient for the buffer and k_{O} refers to the reaction through solvent-related species.

$$k_{\text{obs}}^s = k_{\text{O}} + k_{\text{C}}[\text{buffer}] \quad (1)$$

When the corresponding k_{C} values are plotted against the molar fraction of free acid x_{HA} a nonlinear plot results (Figure 3), which might indicate that even at these (high) pHs the catalysis by H_3PO_4 contributes significantly. In this case, the observed second-order catalytic rate coefficient for the buffer k_{C} is given by eq 2, where K_1 and K_2 are the first and second ionization constants for H_3PO_4 .

$$k_{\text{C}} = k_{\text{H}_3\text{PO}_4} \frac{[\text{H}^+]^2}{[\text{H}^+]^2 + K_1[\text{H}^+] + K_1K_2} + k_{\text{H}_2\text{PO}_4^-} \frac{K_1[\text{H}^+]}{[\text{H}^+]^2 + K_1[\text{H}^+] + K_1K_2} \quad (2)$$

(5) Supporting Information: see paragraph at the end of this paper regarding availability.

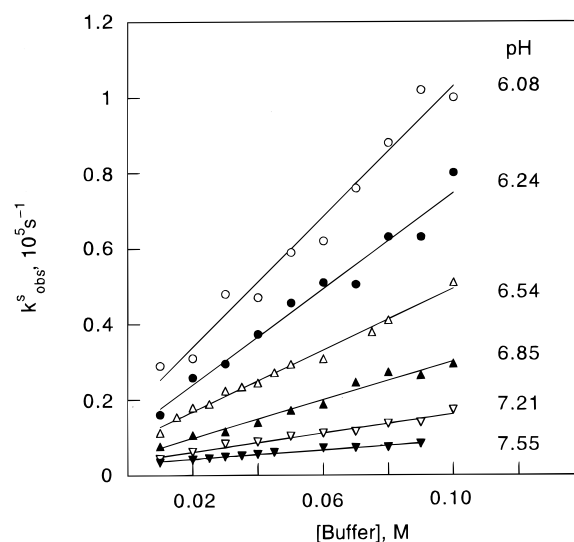


Figure 2. Buffer concentration dependence of the observed rate constant for the slower process in the cis-to-trans isomerization of **DPT** in phosphate buffer.

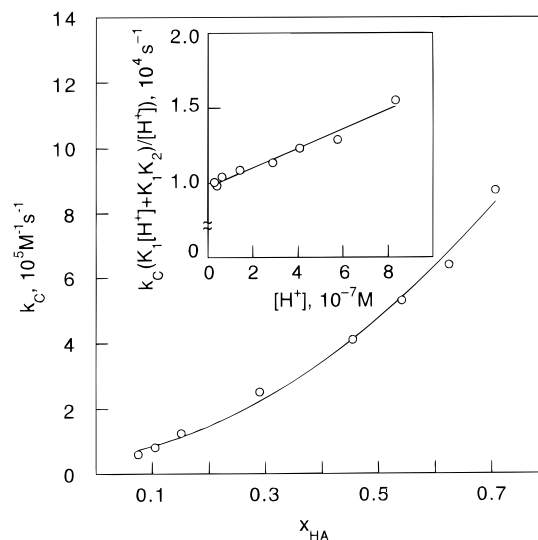


Figure 3. Plot of catalytic rate constant vs molar fraction of acid for cis-to-trans isomerization of **DPT** in phosphate buffer. Inset: plot of left-hand side of eq 3 (see text) vs $[\text{H}^+]$.

Under the experimental conditions of this work, the term $[\text{H}^+]^2$ is negligible in the denominator of eq 2; thus, the latter can be rearranged to eq 3.

$$k_{\text{C}} \times \frac{K_1[\text{H}^+] + K_1K_2}{[\text{H}^+]} = k_{\text{H}_3\text{PO}_4} [\text{H}^+] + K_1k_{\text{H}_2\text{PO}_4^-} \quad (3)$$

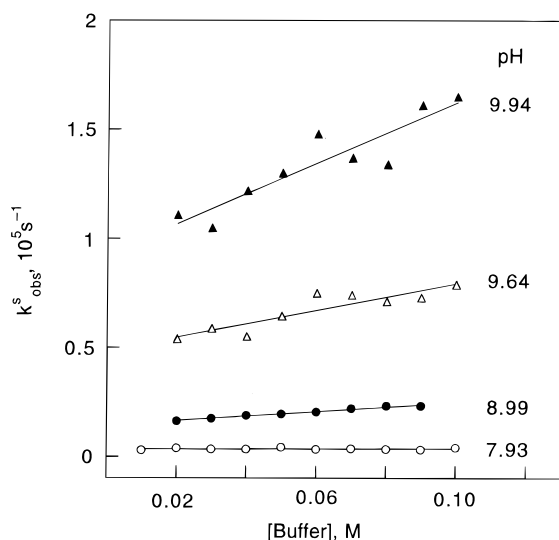
A plot of the left-hand side of eq 3 vs $[\text{H}^+]$ gives a satisfactory straight line (Figure 3 inset). From the intercept and slope values for this plot $k_{\text{H}_3\text{PO}_4}$ and $k_{\text{H}_2\text{PO}_4^-}$ are obtained (Table 1). We are fully aware that this $k_{\text{H}_3\text{PO}_4}$ value arises from conditions where H_3PO_4 is indeed a minor species, but unfortunately, acid-catalyzed hydrolytic decomposition of **DPT** precluded accurate measurements at pH < 6.⁶

Borate Buffer (7.9 < pH < 9.9). As in the case of phosphate buffer, recovery traces are adequately described by two exponential terms with preexponential factors independent of pH and buffer concentration. The

Table 1. Catalytic Rate Constants for Cis-to-Trans Isomerization of DPT in Aqueous Solution^a

acid ^b	$k_{\text{acid}}, \text{M}^{-1} \text{s}^{-1}$	base ^c	$k_{\text{base}}, \text{M}^{-1} \text{s}^{-1}$
H ₃ PO ₄ (1.9 ^d)	$(6.4 \pm 0.7) \times 10^9$	H ₂ BO ₃ ⁻ (8.94 ^e)	$(1.1 \pm 0.1) \times 10^5$
H ₂ PO ₄ ⁻ (6.46 ^e)	$(7.8 \pm 0.3) \times 10^5$	CO ₃ ²⁻ (9.76 ^e)	$(5.9 \pm 0.4) \times 10^5$
		HBO ₃ ²⁻ (11.6 ^e)	$(2.8 \pm 0.3) \times 10^7$

^a At 21 °C, $\mu = 0.5 \text{ M}$ (NaCl). ^b $\text{p}K_{\text{a}}$ given in parentheses. ^c $\text{p}K_{\text{a}}$ of conjugate acid given in parentheses. ^d Taken from ref 28. ^e Determined potentiometrically.

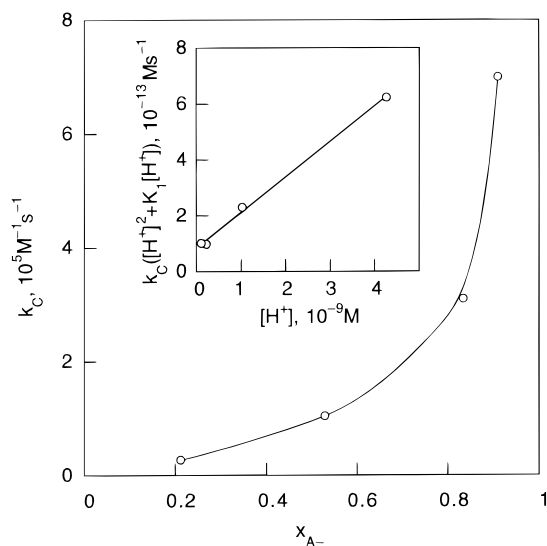
**Figure 4.** Buffer concentration dependence of the observed rate constant for the slower process in the cis-to-trans isomerization of DPT in borate buffer.

observed rate constant corresponding to the faster process (k_{obs}^f) is also found to be independent of pH and buffer concentration (Table S3)⁵ and has an average value of $(3.32 \pm 0.04) \times 10^5 \text{ s}^{-1}$. The observed rate constant corresponding to the slower process (k_{obs}^s), on the other hand, increases as pH and buffer concentration increase as well (Table S4),⁵ which is indicative of base catalysis, with the exception of data at $\text{pH} = 7.93$, which are independent of buffer concentration. Plots of k_{obs}^s vs buffer concentration are fairly linear (Figure 4 is representative), in agreement with eq 1. When the corresponding k_{C} values are plotted against the molar fraction of free base x_{A^-} a nonlinear plot results (Figure 5), which might indicate that even at these (low) pHs the catalysis by HBO_3^{2-} contributes significantly. In this case, the observed second-order catalytic rate coefficient for the buffer k_{C} is given by eq 4, where K_1 and K_2 are the first and second ionization constants for H_3BO_3 .

$$k_{\text{C}} = k_{\text{H}_2\text{BO}_3^-} \frac{K_1[\text{H}^+]}{[\text{H}^+]^2 + K_1[\text{H}^+] + K_1K_2} + k_{\text{HBO}_3^{2-}} \frac{K_1K_2}{[\text{H}^+]^2 + K_1[\text{H}^+] + K_1K_2} \quad (4)$$

Under the experimental conditions of this work, the term K_1K_2 is negligible in the denominator of eq 4; thus, the latter can be rearranged to eq 5.

$$k_{\text{C}}([\text{H}^+]^2 + K_1[\text{H}^+]) = \frac{k_{\text{H}_2\text{BO}_3^-}K_1[\text{H}^+] + K_1K_2k_{\text{HBO}_3^{2-}}}{[\text{H}^+]^2 + K_1[\text{H}^+]} \quad (5)$$

**Figure 5.** Plot of catalytic rate constant vs molar fraction of base for cis-to-trans isomerization of DPT in borate buffer. Inset: plot of left-hand side of eq 5 (see text) vs $[\text{H}^+]$.

A plot of the left-hand side of eq 5 vs $[\text{H}^+]$ gives a satisfactory straight line (Figure 5 inset). From the intercept and slope values for this plot $k_{\text{H}_2\text{BO}_3^-}$ and $k_{\text{HBO}_3^{2-}}$ are obtained (Table 1).

Carbonate Buffer (8.8 < pH < 10.9). At $\text{pH} < 10.0$ recovery traces are adequately described by two exponential terms with preexponential factors independent of pH and buffer concentration. The observed rate constant corresponding to the faster process (k_{obs}^f), as in the case of the other two buffer systems described above, is found to be independent of pH and buffer concentration (Table S5)⁵ and has an average value of $(3.28 \pm 0.04) \times 10^5 \text{ s}^{-1}$. The observed rate constant corresponding to the slower process (k_{obs}^s), on the other hand, increases as pH and buffer concentration increase as well (Table S6),⁵ indicative of base catalysis as observed with borate buffer. Plots of k_{obs}^s vs buffer concentration are fairly linear (Figure 6 is representative), once again, in agreement with eq 1. When the corresponding k_{C} values are plotted against the molar fraction of free base x_{A^-} a linear plot (with negligible intercept) results (Figure 6 inset); from the slope of this plot $k_{\text{CO}_3^{2-}}$ is obtained (Table 1).

At $\text{pH} > 10.0$ recovery traces are adequately described by a single-exponential function. The corresponding observed rate constants (Table S7)⁵ are essentially independent of buffer concentration, and despite a slight increase with pH, they are in very good agreement with the k_{obs}^f values corresponding to the buffer systems described above.

NaOH Buffer (0.005 M ≤ [HO⁻] ≤ 0.20 M). Recovery traces are very well reproduced by a single-exponential function. Observed rate constants are independent of hydroxide ion concentration (Table S8),⁵ and the average value, namely $(3.39 \pm 0.05) \times 10^5 \text{ s}^{-1}$, is in excellent agreement with the values corresponding to k_{obs}^f in the buffer systems described above.

pH Profile. The intercepts of all buffer dependence plots (i.e., k_0 in eq 1) are well defined, and they provide

(6) Triazenes are very sensitive to acids, decomposing in aqueous media to nitrogen, amines and alcohols/phenols. The rate constant determined for proton-catalyzed decomposition of DPT under the experimental conditions of this work is $(1.37 \pm 0.03) \times 10^3 \text{ M}^{-1} \text{ s}^{-1}$ (ref 8).

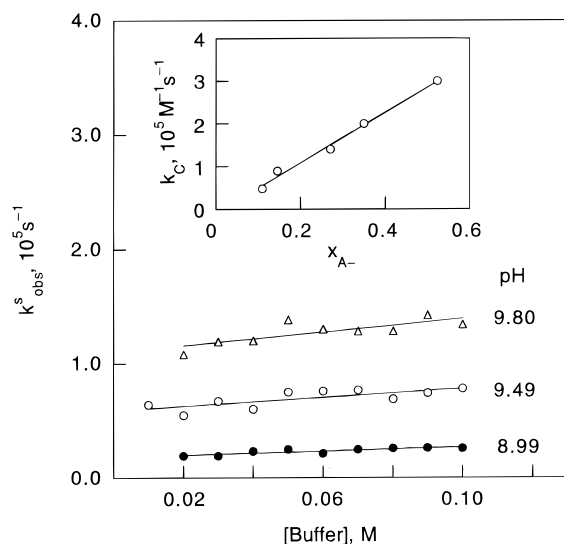


Figure 6. Buffer concentration dependence of the observed rate constant for the slower process in the *cis*-to-*trans* isomerization of **DPT** in carbonate buffer. Inset: catalytic rate constant vs molar fraction of base.

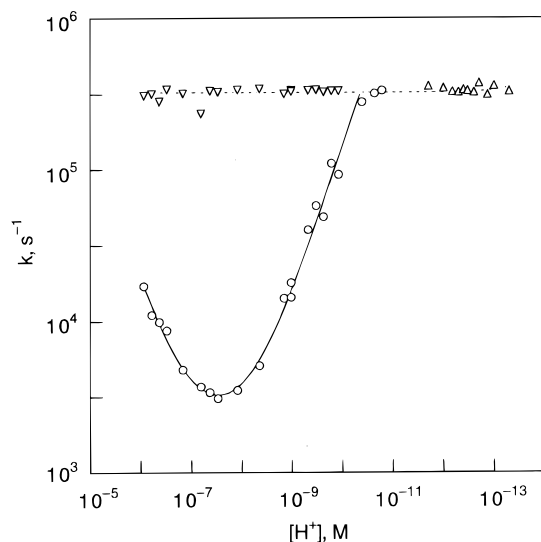


Figure 7. Rate profile for *cis*-to-*trans* isomerization of **DPT** in aqueous solution: \circ , rate constants for reaction through solvent-related species (obtained from the intercept of buffer dependence plots for phosphate, borate and carbonate buffers); ∇ , observed rate constants for faster process detected at $\text{pH} < 10$ in phosphate, borate and carbonate buffers; Δ , observed rate constants for single process detected in NaOH buffer.

rate coefficients for *cis*-to-*trans* isomerization of **DPT** through solvent-related species. The resulting k_0 values and the observed rate constants measured in NaOH buffer are displayed in the rate profile shown in Figure 7; the latter also displays the observed rate constants for the faster process observed at $\text{pH} < 10$. The pH -rate curve corresponding to isomerization through solvent-related species is characterized by a V-shaped profile (with a hardly discernible horizontal section) and a downward bend at pH ca. 10.5. Downward bends of this type are generally interpreted as a result of either a change in the state of ionization of the substrate or a change in rate-controlling step.⁷ Taking into account that

(i) the rate constant for the horizontal segment at $\text{pH} > 10$ (dashed line in Figure 7) is, within experimental errors, *identical* to the values determined for k_{obs}^f at $\text{pH} < 10$, (ii) the preexponential factors for the two first-order processes observed at $\text{pH} < 10$ are independent of pH , (iii) a change in the ionization state of the substrate requires the point of intersection of the two arms of the profile to occur 0.301 units above the pH -rate curve (not the case of Figure 7), and (iv) *cis*-**DPT** is indeed expected to be less acidic than *trans*-**DPT** (see below), the downward bend shown in Figure 7 is ascribed to a change in rate-controlling step.

The empirical rate law for the rate profile corresponding to k_0 at $\text{pH} < 10$ consists of three terms as given in eq 6, each term representing a different mechanism.⁷

$$k_0 = c_1[\text{H}^+] + c_2 + c_3[\text{HO}^-] \quad (6)$$

The first term of eq 6 represents the left-hand side of the V-shaped profile which gives way to a diagonal portion of slope = -1, signifying acid catalysis. The second term is attributable to an "uncatalyzed" reaction. Finally, the third term represents the right-hand side of the V-shaped profile, which gives way to a diagonal portion of slope = 1, signifying base catalysis. Analysis by least-squares fitting according to eq 6 (solid line in Figure 7) leads to values of $(1.3 \pm 0.1) \times 10^{10} \text{ M}^{-1} \text{ s}^{-1}$, $(2.2 \pm 0.2) \times 10^3 \text{ s}^{-1}$, and $(1.5 \pm 0.1) \times 10^9 \text{ M}^{-1} \text{ s}^{-1}$ for c_1 to c_3 , respectively.

Discussion

The $\text{p}K_a$ for *trans*-**DPT** determined under the experimental conditions of this work is (13.0 ± 0.1) ,⁸ in good agreement with the reported value in 20% ethanol aqueous solution, namely (13.26 ± 0.04) .⁹ Not surprisingly, **DPT** is a significantly stronger acid than aniline ($\text{p}K_a \sim 27$ at 25 °C),¹⁰ owing to the electron-withdrawing character (i.e. inductive and resonance effects) of the $\text{PhN}=\text{N}-$ group. In the case of *cis*-**DPT**, one would anticipate resonance delocalization to be more restricted as a result of steric hindrance, and consequently, the $-\text{NH}-$ group of *cis*-**DPT** is expected to be less acidic than that in the *trans* isomer. For comparative purposes, it should be pointed out here that the *cis* isomers of 2-hydroxy-5-methylazobenzene ($\text{p}K_a = 10.7$)¹¹ and 4-[4'-(dimethylamino)phenylazo]benzenesulfonate ($\text{p}K_a = 5.0$)¹² have indeed been shown to be significantly weaker acids than the corresponding *trans* forms ($\text{p}K_a = 9.4$ ¹¹ and 2.70 ¹³– 2.87 ,¹⁴ respectively). Thus, laser excitation of *trans*-**DPT** under the experimental conditions of this work would result in instantaneous formation of neutral *cis*-**DPT**.

The kinetic data presented in the previous section can be interpreted in terms of the general mechanism shown in eq 7, where **A** and **B** represent neutral *cis*-**DPT** forms,

(8) Chen, N. M. Sc., University of Waterloo, 2000.

(9) Benes, J.; Beránek, V.; Zimprich, J.; Vetesnik, P. *Collect. Czech. Chem. Commun.* **1977**, *42*, 702.

(10) Albert, A.; Serjeant, E. P. *The Determination of Ionization Constants*, 3rd ed.; Chapman & Hall: New York, 1984; p 149.

(11) Wettermark, G.; Langmuir, M. E.; Anderson, D. G. *J. Am. Chem. Soc.* **1965**, *87*, 476.

(12) Sanchez, A. M.; Barra, M.; de Rossi, R. H. *J. Org. Chem.* **1999**, *64*, 1604.

(13) Tawarah, K. M.; Abu-Shamleh, H. M. *Dyes Pigments* **1991**, *16*, 241.

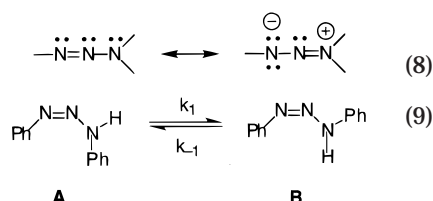
(14) Reeves, R. L. *J. Am. Chem. Soc.* **1966**, *88*, 2240.

(7) Loudon, G. M. *J. Chem. Educ.* **1991**, *68*, 973.

and the second step corresponds to the thermal cis-to-trans isomerization catalyzed by general acids or general bases.



It is well-known that rotation around the nitrogen–nitrogen single bond of triazenes has a relatively high free energy barrier, which is ascribed to the partial double bond character that results from 1,3-dipolar contributions (eq 8).^{15–21} Hence, *cis*-DPT is proposed to exist as a pair of rotamers (eq 9) which are expected to undergo cis-to-trans isomerization at different rates as a result of stereoelectronic factors. In fact, based on the 1,3-hydrogen shift mechanisms shown in Scheme 1 rotamer **B** is predicted to isomerize more rapidly than rotamer **A**.



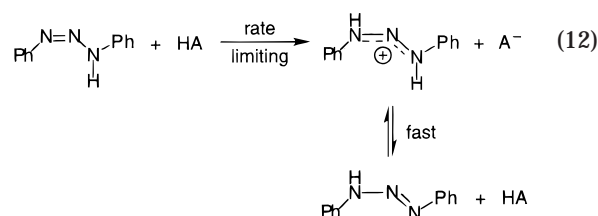
As already mentioned, two well-distinguishable processes are observed at pH < 10. The faster process, independent of pH and buffer concentration, is ascribed to the interconversion of cis rotamers (i.e., eq 9), and the corresponding observed rate constant k_{obs}^f is given by eq 10. The second process detected, catalyzed by general acids or general bases, is ascribed to the thermal cis-to-trans isomerization and the corresponding observed rate constant k_{obs}^s is given by eq 11, where $K_1 = k_1/k_{-1}$, and $k_{\text{H}_2\text{O}}$, k_{acid} , and k_{base} represent the uncatalyzed and acid/base catalytic rate coefficients, respectively.

$$k_{\text{obs}}^f = k_1 + k_{-1} \quad (10)$$

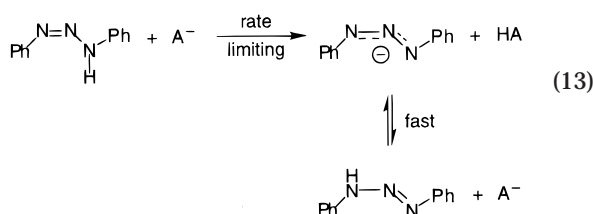
$$k_{\text{obs}}^s = \frac{K_1}{1 + K_1} (k_{\text{H}_2\text{O}} + \sum k_{\text{acid}}[\text{acid}] + \sum k_{\text{base}}[\text{base}]) \quad (11)$$

No evidence of concerted acid/base-catalysis, as might be expected from mechanism (b) in Scheme 1, was obtained under the experimental conditions of this work. The general acid-catalyzed mechanism is interpreted as shown in eq 12, and involves rate-determining proton transfer to the nitrogen–nitrogen double bond of rotamer **B** to give a resonance-stabilized cation, which then loses a proton from the position that gives the thermodynamically more stable *trans*-triazene. This mechanism is

analogous to the acid-catalyzed enol-ketonization mechanism²² and to the acid-catalyzed double-bond rearrangement of alkenes.²³



The general base-catalyzed mechanism, on the other hand, is interpreted as represented by eq 13 and involves rate-determining base-promoted ionization of the amino nitrogen of rotamer **B** to give a resonance-stabilized anion, which then combines with a proton at the position that gives the thermodynamically more stable *trans*-triazene. This mechanism resembles the base-catalyzed enolization process²² as well as the base-catalyzed double-bond rearrangement of alkenes.²³



The “uncatalyzed” process (i.e., c_2 in eq 6) would correspond to solvent water molecules acting as proton donors (eq 12) or as basic proton acceptors (eq 13). Evidently, prototropic rearrangements of the type shown in eqs 12 and 13 do not lead to a change in the nitrogen–nitrogen double bond configuration when applied to rotamer **A**.

At high pH, the interconversion of rotamers becomes rate-controlling, and only one process is detected. The fact that the rate constants observed with NaOH buffer are *identical* to the k_{obs}^f values determined at pH < 10 would indicate that k_{-1} is indeed significantly smaller than k_1 (i.e., eq 10 simplifies to $k_{\text{obs}}^f = k_1$) and $K_1 = k_1/k_{-1} \gg 1$. This observation is consistent with the relative stability predicted for this pair of rotamers (i.e., **A** less stable than **B**). Thus, the factor $K_1/(1 + K_1)$ in eq 11 is for practical purposes unity, and the coefficients c_1 to c_3 in eq 6 would correspond, respectively, to k_{H^+} , $k_{\text{H}_2\text{O}}$, and k_{HO^-} in eq 11. In fact, the catalytic rate coefficients thus ascribed to H^+ and HO^- are consistent with diffusion-controlled protonation rate constants.²⁴

To the best of our knowledge, no energy barrier for hindered rotation around the nitrogen–nitrogen single bond in disubstituted triazenes has been determined so far. Nonetheless, one would anticipate a higher free energy of activation for the cis isomer relative to the trans form due to steric interactions. Based on the application of the Eyring equation²⁵ to k_1 , a value of $3.3 \times 10^5 \text{ s}^{-1}$ (at 21 °C) for this rate constant would correspond to a free

(15) Marullo, N. P.; Mayfield, C. B.; Wagener, E. H. *J. Am. Chem. Soc.* **1968**, *90*, 510.

(16) Akhtar, M. H.; McDaniel, R. S.; Feser, M.; Oehlschlager, A. C. *Tetrahedron* **1968**, *24*, 3899.

(17) Lunazzi, L.; Cerioni, G.; Foresti, E.; Macciantelli, D. *J. Chem. Soc., Perkin Trans. 2* **1978**, 686.

(18) Sieh, D.; Wilbur, D. J.; Michejda, C. J. *J. Am. Chem. Soc.* **1980**, *102*, 3883.

(19) Golding, B. T.; Kemp, T. J.; Narayanaswamy, R.; Waters, B. W. *J. Chem. Res., Synop.* **1984**, 130.

(20) Lippert, Th.; Wokaun, A.; Dauth, J.; Nuyken, O. *Magn. Reson. Chem.* **1992**, *30*, 1178.

(21) Panitz, J.-C.; Lippert, Th.; Stebani, J.; Nuyken, O.; Wokaun, A. *J. Phys. Chem.* **1993**, *97*, 5246.

(22) Toullec, J. *Adv. Phys. Org. Chem.* **1982**, *18*, 1.

(23) Mackenzie, K. in *The Chemistry of Alkenes*; Patai, S., Ed.; John Wiley & Sons: London, 1964; Vol. 1, Chapter 7.

(24) Eigen, M. *Angew. Chem., Int. Ed. Engl.* **1964**, *3*, 1.

(25) Lowry, T. H.; Richardson, K. S. *Mechanisms and Theory in Organic Chemistry*; Harper & Row: New York, 1987; p 209.

energy of activation of ca. 9.8 kcal/mol. This value is comparable to the free energy barriers typically determined for hindered rotation in trisubstituted triazenes in organic solvents, namely 10–20 kcal/mol.^{15–20} On the other hand, an appreciable higher free energy barrier for hindered rotation is expected upon protonation or deprotonation of the triazene moiety, owing to the increase of the partial double bond character as a result of charge delocalization. Thus, interconversion between the corresponding conjugate acids and bases of rotamers **A/B** can be ignored.

In summary, the thermal cis-to-trans isomerization of **DPT** in aqueous solution is found to be catalyzed by general acids and general bases. Catalysis is attributed to acid/base-promoted 1,3-prototropic rearrangements leading to isomerization, consistent with previous studies in protic organic solvents.^{3a,4} In addition, a process characterized by an estimated free energy barrier of 9.8 kcal/mol is also observed. This process is ascribed to the interconversion of neutral cis rotamers through hindered rotation around the nitrogen–nitrogen single bond.

Experimental Section

1,3-Diphenyltriazene (Aldrich) was purified by treatment with Cd(OH)₂ generated in situ from Cd(NO₃)₂ (Allied Chemical) in basic methanol (BDH, ACS grade) aqueous solution, as described in the literature.²⁶ Aqueous buffer solutions were prepared using analytical grade salts and water purified in a Millipore apparatus.

To minimize any acid-catalyzed substrate decomposition, samples were analyzed immediately after adding the substrate dissolved in methanol (BDH, Omnisolv grade) to solutions containing all the other constituents. The total methanol concentration was 2% (by volume), and the ionic strength was kept constant at 0.5 M using NaCl as compensating electrolyte.

(26) Dwyer, F. P. *J. Soc. Chem. Ind. London* **1937**, 56, 70.

(27) Barra, M.; Agha, K. A. *J. Photochem. Photobiol., A: Chem.* **1997**, 109, 293.

(28) Smith, R. M.; Martell, A. E. *Critical Stability Constants*; Plenum Press: New York, 1974; Vol. 6.

(29) Harned, H. S.; Owen, B. B. *The Physical Chemistry of Electrolytic Solutions*; Reinhold Publishing Corp.: New York, 1958; (a) p 748; (b) p 752; (c) p 638.

Laser experiments were carried out using a Q-switched Nd:YAG laser (Continuum, Surelite I) operated at 355 nm (4–6 ns pulses, < 30 mJ/pulse) for excitation. Further details on this laser system have already been reported.^{12,27} Solutions were contained in quartz cells constructed of 7 × 7 mm² Suprasil tubing. Transient absorption spectra were collected under flow conditions in order to ensure the irradiation of fresh portions of sample by each laser pulse. All measurements were carried out at 21 °C.

For each solution, kinetic traces were recorded at 390 nm in different time domains (0.08–8 μs per point) and then combined for analysis; if at all necessary, traces were previously normalized to account for slight differences in signal intensity due to laser power fluctuations. Observed rate constants were determined by using the general curve fitting procedure of Kaleidagraph 3.0.5 software from Abelbeck Software.

Molar fractions were calculated from the observed pH by using the ionization equilibrium constants determined potentiometrically under our experimental conditions, unless stated otherwise. Thus, ionization constants were obtained by extrapolating the pH values of solutions containing the corresponding conjugate acid and base in 1:1 ratio to zero buffer concentration; resulting values are summarized in Table 1 and are in excellent agreement with reported values under similar conditions.²⁸

Proton concentrations for the rate profile (Figure 7) were calculated from the observed pH by using a value of 0.732 for the proton activity coefficient,^{29a} except for data from NaOH buffer. In this case proton concentrations were calculated according to eq 14 using $(\gamma_{\text{H}^+}\gamma_{\text{HO}^-}/a_{\text{H}_2\text{O}}) = 0.516$ ^{29b} and $K_w = 0.6806 \times 10^{-14}$.^{29c}

$$[\text{H}^+] = \frac{K_w}{\gamma_{\text{H}^+}\gamma_{\text{OH}^-}/a_{\text{H}_2\text{O}}} \frac{1}{[\text{OH}^-]} \quad (14)$$

Acknowledgment. This work was supported by research and equipment grants from the Natural Sciences and Engineering Research Council (NSERC) of Canada.

Supporting Information Available: Observed rate constants for thermal cis-to-trans isomerization of 1,3-diphenyltriazene in buffered aqueous solutions as a function of pH and buffer concentration. This material is free of charge via the Internet at <http://pubs.acs.org>.

JO000599L